

Available online at [www.sciencedirect.com](http://www.sciencedirect.com)

# Metabolism

[www.metabolismjournal.com](http://www.metabolismjournal.com)

## Palmitate-induced Activation of Mitochondrial Metabolism Promotes Oxidative Stress and Apoptosis in H4IIEC3 Rat Hepatocytes

Robert A. Egnatchik<sup>a</sup>, Alexandra K. Leamy<sup>a</sup>, Yasushi Noguchi<sup>b</sup>, Masakazu Shiota<sup>c</sup>, Jamey D. Young<sup>a,c,\*</sup>

<sup>a</sup> Chemical and Biomolecular Engineering, Vanderbilt University, Nashville, TN, USA

<sup>b</sup> Institute for Innovation, Ajinomoto Co., Inc., Kawasaki, Japan

<sup>c</sup> Molecular Physiology and Biophysics, Vanderbilt University, Nashville, TN, USA

### ARTICLE INFO

#### Article history:

Received 4 May 2013

Accepted 20 October 2013

#### Keywords:

Lipotoxicity

Metabolic flux analysis

Isotopomer modeling

Mass spectrometry

Reactive oxygen species

### ABSTRACT

**Objective.** Hepatic lipotoxicity is characterized by reactive oxygen species (ROS) accumulation, mitochondrial dysfunction, and excessive apoptosis, but the precise sequence of biochemical events leading to oxidative damage and cell death remains unclear. The goal of this study was to delineate the role of mitochondrial metabolism in mediating hepatocyte lipotoxicity.

**Materials/Methods.** We treated H4IIEC3 rat hepatoma cells with free fatty acids in combination with antioxidants and mitochondrial inhibitors designed to block key events in the progression toward apoptosis. We then applied <sup>13</sup>C metabolic flux analysis (MFA) to quantify mitochondrial pathway alterations associated with these treatments.

**Results.** Treatment with palmitate alone led to a doubling in oxygen uptake rate and in most mitochondrial fluxes. Supplementing culture media with the antioxidant N-acetyl-cysteine (NAC) reduced ROS accumulation and caspase activation and partially restored cell viability. However, <sup>13</sup>C MFA revealed that treatment with NAC did not normalize palmitate-induced metabolic alterations, indicating that neither elevated ROS nor downstream apoptotic events contributed to mitochondrial activation. To directly limit mitochondrial metabolism, the complex I inhibitor phenformin was added to cells treated with palmitate. Phenformin addition eliminated abnormal ROS accumulation, prevented the appearance of apoptotic markers, and normalized mitochondrial carbon flow. Further studies revealed that glutamine provided the primary fuel for elevated mitochondrial metabolism in the

**Abbreviations:** BSA, bovine serum albumin; CAC, citric acid cycle; Eto, etomoxir; FFA, free fatty acid; GC-MS, gas chromatography–mass spectrometry; H<sub>2</sub>DCFDA, 2'-7'-dichlorodihydrofluorescein diacetate; MFA, metabolic flux analysis; MUFA, monounsaturated fatty acid; NAC, N-acetyl cysteine; NAFLD, non-alcoholic fatty liver disease; NASH, non-alcoholic steatohepatitis; OA, oleate; PHEN, phenformin; PA, palmitate; PI, propidium iodide; ROS, reactive oxygen species; SFA, saturated fatty acid.

**Metabolites and enzymes:** AcCoA, acetyl-CoA; AKG, alpha-ketoglutarate; Cit, citrate; Fum, fumarate; Glc, glucose; Glu, glutamate; Gln, glutamine; Lac, lactate; Mal, malate; Net Glyc, net glycolysis; Pyr, pyruvate; Suc, succinate; ADH, alpha-ketoglutarate dehydrogenase; CS, citrate synthase; GLN, glutamine uptake; ME, malic enzyme; PC, pyruvate carboxylase.

\* Corresponding author. Chemical and Biomolecular Engineering, VU Station B 351604. Tel.: +1 615 343 4253; fax: +1 615 343 7951.

E-mail address: [j.d.young@vanderbilt.edu](mailto:j.d.young@vanderbilt.edu) (J.D. Young).

presence of palmitate, rather than fatty acid beta-oxidation, and that glutamine consumption could be reduced through co-treatment with phenformin but not NAC.

**Conclusion.** Our results indicate that ROS accumulation in palmitate-treated H4IIEC3 cells occurs downstream of altered mitochondrial oxidative metabolism, which is independent of beta-oxidation and precedes apoptosis initiation.

© 2014 Elsevier Inc. All rights reserved.

## 1. Introduction

There are currently two competing views on the role of lipid beta-oxidation in the development of non-alcoholic fatty liver disease (NAFLD) [1,2]. One view holds that impaired or incomplete beta-oxidation leads to hepatic steatosis and accumulation of lipid intermediates that inhibit insulin signaling [3,4]. The other view holds that increased supply of free fatty acids (FFAs) to liver results in excessive beta-oxidation that fuels reactive oxygen species (ROS) accumulation and inflammation [5–7]. Recently, isotope tracers and nuclear magnetic resonance (NMR) were applied to determine *in vivo* metabolic fluxes in human subjects with either high or low intrahepatic triglyceride content [2]. It was found that citric acid cycle (CAC) flux was approximately 2-fold greater in NAFLD patients. This increase in mitochondrial activity was associated with a 50% higher rate of systemic lipolysis and a 50% higher rate of hepatic anaplerotic flux, demonstrating that elevated lipid levels strongly impact mitochondrial function in NAFLD patients. Similar metabolic alterations were measured in high-fat diet (HFD) fed mice, which were associated with elevated oxidative stress markers [1]. The authors hypothesized that citric acid cycle (CAC) activation is required to meet energetic demands in the face of reduced respiratory efficiency resulting from mitochondrial oxidative damage. In this contribution, we explore an alternative hypothesis, which is the possibility that FFAs can enhance mitochondrial metabolism independently of beta-oxidation through a mechanism that precedes the onset of oxidative damage.

Our study builds upon an extensive literature that uses hepatic cell lines to mimic the effects of obesity, NAFLD, and non-alcoholic steatohepatitis (NASH) in culture [8–12]. Studying the effects of lipid oversupply in cultured cells is useful because it enables complete control of the cellular environment to examine basic biochemical mechanisms of hepatic lipotoxicity. In this context, saturated fatty acid (SFA) treatments lead to acute lipotoxicity that is associated with increased ROS and endoplasmic reticulum (ER) stress but is independent of ceramide synthesis [9,13,14]. Furthermore, the response to SFA treatment is altogether different from that of monounsaturated fatty acid (MUFA) treatment, which induces steatotic triglyceride formation without initiating ROS accumulation or apoptosis [15]. Therefore, modulating the FFA composition of the culture medium can be used to achieve varied outcomes ranging from progressive lipotoxicity to benign steatosis.

Prior *in vitro* experiments have attributed the onset of SFA-induced oxidative stress to activation of NADPH oxidases [16] or increased fatty acid beta-oxidation [8]. In the mitochondria, loss of electrons from complexes I and III of the electron transport chain (ETC) can combine with oxygen to generate

ROS, which include superoxide ions, hydroxyl radicals, and hydrogen peroxide [17]. ROS are powerful oxidizing agents that indiscriminately damage many important components of the cell including DNA, lipid membranes, and proteins [18]. At high levels, ROS are known to activate pro-apoptotic pathways, thus initiating programmed cell death. ROS accumulation can trigger apoptosis through c-Jun N-terminal kinase (JNK) stress signaling pathways [19]. Antioxidant co-treatments have been shown to prevent JNK phosphorylation and JNK-mediated insulin resistance in SFA-treated H4IIEC3 cells [8]. Co-treatment with a radical scavenger also prevented HepG2 human hepatoma cell death in the presence of elevated palmitate [20]. These prior studies indicate that ROS accumulation is potentially a committed step in the lipotoxicity mechanism, and that JNK activation may be one mechanism by which ROS accumulation initiates apoptosis [8,10]. However, the role of specific metabolic pathways in promoting ROS accumulation, as well as the mechanism of their dysregulation by palmitate, remains largely undefined.

Stable isotope-based metabolic flux analysis (MFA) has been previously applied to study how elevated SFAs impact central metabolism in hepatic cells [9]. Detailed flux mapping with [ $U$ - $^{13}C_5$ ]glutamine revealed that palmitate treatment strongly increased CAC fluxes relative to glycolytic fluxes in H4IIEC3 cells. Changes in intracellular metabolic fluxes coincided with the onset of ROS accumulation and preceded the appearance of apoptotic markers such as caspase 3/7 activation and DNA laddering. The same study showed that oleate co-treatment led to a reversal of the palmitate-induced metabolic phenotype and completely rescued H4IIEC3 cells from apoptosis, which was likely a result of enhanced partitioning of palmitate into triglyceride stores. Together with the previously described human and mouse data, these studies suggest that mitochondrial dysregulation arising from increased FFA availability plays a key role in both *in vitro* and *in vivo* lipotoxicity mechanisms, but they do not directly assess whether enhanced mitochondrial metabolism is a cause or a consequence of other lipotoxic effects such as oxidative stress or apoptosis initiation. Furthermore, they do not conclusively define whether FFAs are acting primarily as a fuel substrate to activate CAC flux.

To address these questions, we applied  $^{13}C$  MFA in combination with treatments designed to alter ROS accumulation and mitochondrial metabolism in H4IIEC3 rat hepatoma cells fed lipotoxic concentrations of the SFA palmitate. These studies revealed that palmitate increased oxygen consumption and CAC fluxes independently of fatty acid beta-oxidation. Glutamine, rather than lipid, was the preferred substrate used to fuel palmitate-induced increases in mitochondrial metabolism. Co-treating cells with the antioxidant *N*-acetyl cysteine (NAC) prevented ROS accumulation and caspase activation in

the presence of palmitate but did not reverse the palmitate-associated metabolic phenotype. On the other hand, direct inhibition of mitochondrial metabolism with the complex I antagonist phenformin abolished palmitate-associated flux alterations while reversing other lipotoxicity markers. The results indicate that palmitate-induced dysregulation of mitochondrial oxidative metabolism is the primary cause of ROS accumulation and apoptosis in H4IIEC3 cells. Interestingly, these metabolic alterations are independent of fatty acid beta-oxidation and precede the onset of oxidative damage or apoptosis initiation.

## 2. Materials and Methods

### 2.1. Materials

Palmitate, oleate, bovine serum albumin, phenformin, N-acetyl cysteine, low glucose Dulbecco's modified Eagle's medium (DMEM), and etomoxir were purchased from Sigma (St. Louis, MO, USA). AICAR was purchased from Cayman Chemicals (Ann Arbor, MI, USA). Propidium iodide (PI) and 2',7'-dichlorodihydrofluorescein diacetate (H<sub>2</sub>DCFDA) were purchased from Invitrogen (Carlsbad, CA, USA).

### 2.2. Cell culture

The H4IIEC3 rat hepatoma cell line (American Type Culture Collection, Manassas, VA, USA) was cultured in low glucose DMEM supplemented with 10% FBS and 1% penicillin/streptomycin antibiotic solution. The glutamine concentration of the culture medium was 2 mmol/L. For fluorescence-based assays, cells were seeded in 96-well plates at  $2 \times 10^4$  cells per well two days prior to experiments to achieve 80%–90% confluency at the time of measurement.

### 2.3. Preparation of fatty acid solutions

FFA stock solutions were prepared by coupling free fatty acids with bovine serum albumin (BSA). First, palmitate or oleate was dissolved in pure ethanol at a concentration of 195 mmol/L so that the final concentration of ethanol in our FFA stock solutions did not exceed 1.5% by volume. This FFA stock solution was then added to a prewarmed 10% w/w BSA solution (37 °C) to achieve a final FFA concentration of 3 mmol/L, and this solution was allowed to incubate in a water bath for an additional 10 min. The final ratio of FFA to BSA was 2:1. All vehicle treatments were prepared using stocks of 10% w/w BSA with an equivalent volume of ethanol added to match the concentration in FFA stocks. The final concentration of ethanol in all experimental treatments was less than 0.2% by volume.

### 2.4. Detection of ROS

The radical-sensitive H<sub>2</sub>DCFDA dye was used to monitor intracellular ROS production. Cells were seeded on 96-well plates at  $2 \times 10^4$  cells per well. After treatment with fatty acids and/or inhibitors, cells were washed twice with Hank's Balanced Saline Solution (HBSS) and then incubated with

10 μmol/L H<sub>2</sub>DCFDA for one hour at 37 °C in the dark. Oxidation of the dye by intracellular ROS generates a fluorescent 2,7-dichlorofluorescein (DCF) signal. Fluorescence was measured using the excitation/emission wavelengths 485/530 nm with a Biotek FL600 microplate reader.

### 2.5. Viability/Toxicity assays

Cell viability was measured using the Promega Cell Titer Blue kit at 24 h (Fitchburg, WI, USA). Cells were washed twice with HBSS and incubated with dye for 4 h at 37 °C. The kit measures viability by quantifying resazurin reduction, which indicates metabolic production of reducing equivalents. Fluorescence was measured using the excitation/emission wavelengths 530/590 nm with a Biotek FL600 microplate reader. Additionally, we assessed cell toxicity using the dead-cell stain propidium iodide (PI). PI is an intercalating dye that becomes highly fluorescent with excitation wavelength of 530 nm and emission wavelength of 645 nm when embedded in the exposed double-stranded DNA of dead cells.

### 2.6. Caspase activity

The Apo-ONE Homogenous Caspase 3/7 Assay kit was used to measure the activities of caspases 3 and 7 as markers of apoptosis. H4IIEC3 hepatoma cells were cultured in 96-well plates as described previously. Cells were then incubated with designated treatments for at least 6 h. The Apo-ONE kit uses a lysis buffer combined with a caspase 3/7 specific substrate. This substrate, Z-DEVD-R110, becomes fluorescent once its DEVD peptide is removed by the caspases. Fluorescence is then measured at an excitation wavelength of 485 nm and emission wavelength at 530 nm. Caspase 3/7 activation is known to be a reliable indicator of apoptosis initiation in palmitate-treated H4IIEC3 cells, as shown in several previous reports using the Apo-ONE assay in combination with additional apoptosis markers such as DNA laddering or cytochrome C release [9,21].

### 2.7. Metabolite extraction and GC-MS analysis of <sup>13</sup>C labeling

The extraction of intracellular metabolites from H4IIEC3 rat hepatomas and GC-MS analysis of <sup>13</sup>C labeling from [U-<sup>13</sup>C<sub>5</sub>] glutamine or [U-<sup>13</sup>C<sub>16</sub>]palmitate were performed as described previously [9]. Briefly, cell metabolism was quenched by adding 1 mL of pre-cooled methanol (–80 °C) to cultured cells in 10-cm dishes. A biphasic extraction was used to separate polar metabolites into a methanol/water phase and non-polar metabolites into a chloroform phase. Note that this extraction results in mixing of free metabolites from separate subcellular compartments. Polar metabolites were converted to their tert-butylsilyl derivatives using MBTSTFA + 1% TBDMCS (Pierce). Then, 1 μL of each derivitized sample was injected into an Agilent 6890 N/5975B GC-MS equipped with a 30 m DB-35 ms capillary column for analysis of isotopic enrichment.

### 2.8. Oxygen consumption

Oxygen uptake flux was used as a direct measurement of mitochondrial metabolism. These experiments were

performed using the Oroboros Oxygraph-2K, which contains two chambers with separate oxygen probes to monitor on-line changes in oxygen concentration. The instrument was set to a temperature of 32 °C, and the stirring speed for each chamber was 750 rpm. To perform these experiments, H4IIEC3 cells were cultured on 10-cm dishes until 80%–90% confluent and subsequently incubated with selected combinations of fatty acids and treatments for 3 h. Cells were then trypsinized, counted, and resuspended in the same culture medium at a concentration of 2 million cells per mL. Following resuspension, 2 million cells were injected into the Oxygraph instrument.

### 2.9. Beta-oxidation measurements

Cell cultures fed tritiated fatty acid produce  $^3\text{H}_2\text{O}$  at a rate proportional to that of mitochondrial beta-oxidation. Albumin-bound [9,10- $^3\text{H}(\text{N})$ ] palmitic acid (4  $\mu\text{Ci } ^3\text{H}/\mu\text{mol}$  palmitate) was added to cells grown to confluency in 6-well dishes at a final concentration of 400  $\mu\text{mol/L}$ . The final volume of the media solution, including culture medium with glucose and glutamine, inhibitors/activators, and palmitate, was calculated to be exactly 2 mL per well. After 6 h of incubation, 1.5 mL of media was removed directly from each well and collected in individual round-bottom snap-top tubes. Then 75  $\mu\text{L}$  of 60% perchloric acid was added to each sample for deproteinization and to remove albumin-bound unoxidized palmitate from the sample media. The deproteinization reaction was allowed to continue overnight at 4 °C.

Following deproteinization, samples were centrifuged for 30 min. Then, 1.2 mL of sample was collected into a new centrifuge tube and 5  $\mu\text{L}$  of pH indicator dye and 36  $\mu\text{L}$  of 5 M  $\text{K}_2\text{CO}_3$  were added for neutralization. This reaction was allowed to continue overnight at 4 °C. After neutralization, samples were centrifuged for 30 min. To remove any remaining palmitate, 0.8 mL of neutralized sample was applied to an individual AG 1-X8 Resin (BioRad, Hercules, CA) column, and the column was allowed to empty under gravity flow. Each column was flushed twice with 0.6 mL of distilled water. The initial charge (0.8 mL) and all subsequent washes (1.2 mL) were collected in a scintillation vial (PerkinElmer, Waltham, MA). 10 mL of EcoLite scintillation cocktail fluid (MP Biomedical, Santa Ana, CA) was added to each sample vial, shaken vigorously, and read in a scintillation counter.

### 2.10. Metabolic flux analysis

Feeding cells [ $\text{U-}^{13}\text{C}_5$ ]glutamine isotope tracer results in unique isotopic enrichment patterns in downstream metabolites dependent on the intracellular metabolism [22]. It is therefore possible to evaluate the intracellular fluxes that give rise to the measured enrichment patterns by minimizing the lack of fit between measured and simulated mass isotopomer distributions derived from a mathematical model of the metabolic reaction network. We performed  $^{13}\text{C}$  MFA on H4IIEC3 rat hepatomas under several treatment conditions in the presence of glucose using custom Matlab-based software that relies on an elementary metabolite unit (EMU) decomposition to efficiently simulate mass isotopomer distributions of intracellular metabolites [23,24]. We constructed an isotopomer

model to simulate labeling from [ $\text{U-}^{13}\text{C}_5$ ]glutamine into glutamate, pyruvate, lactate, and several CAC intermediates, which was qualitatively similar to a previous model developed by Noguchi et al. [9]. The flux parameters of the model were iteratively adjusted using a Levenberg–Marquardt algorithm until optimal agreement with experimental data was obtained. Flux estimation was repeated a minimum of 50 times from random initial values to ensure a global minimum was achieved. All results were subjected to a chi-square statistical test to assess goodness-of-fit ( $\chi = 0.01$ ), and accurate 95% confidence intervals were computed for all estimated parameters by evaluating the sensitivity of the sum-of-squared residuals to parameter variations [25]. A detailed description of the reaction network and modeling assumptions can be found in the Supplementary Materials.

### 2.11. Statistical analysis

Tests for statistical significance were performed using analysis of variance (Model I ANOVA) and Tukey–Kramer methods for multiple comparisons, or Student's t-test for pair-wise comparisons. Plots indicate  $\pm$  one standard error of the mean unless otherwise indicated.

---

## 3. Results

### 3.1. Palmitate overload promotes ROS accumulation and apoptosis

In this study, H4IIEC3 cells were incubated with 400  $\mu\text{mol/L}$  palmitate (PA) as a model of SFA-induced lipotoxicity, consistent with previous studies [9]. We have chosen to use the H4IIEC3 rat hepatoma cell line because it has been used in several hallmark papers on the subject of hepatic lipotoxicity and has been shown to accurately recapitulate the response of primary hepatocytes to an elevated PA load [8,9,11]. A dose of 400  $\mu\text{mol/L}$  PA was selected to maintain consistency with these prior studies. We confirmed this dose by subjecting H4IIEC3 cells to increasing concentrations of PA and found that 400  $\mu\text{mol/L}$  palmitate provided the maximum lipotoxic effect while remaining in a physiologically relevant range (Supplementary Fig. S1). After 6 h of treatment, PA-treated cells exhibited a significant increase in ROS accumulation as measured by DCF fluorescence (Fig 1A). Additionally, PA-treated cells were marked by elevated caspase 3/7 activity at 12 h (Fig. 1B). After 24 h of PA treatment, cell viability was reduced by approximately two-thirds in comparison to the vehicle-treated (BSA) control group (Fig. 1C). In contrast, cells treated with the same concentration of oleate (OA) did not exhibit markers of oxidative stress or apoptosis (Fig. 1 A, B, C).

### 3.2. Palmitate stimulates mitochondrial oxidative metabolism

ROS can be produced due to accelerated flux of electrons through the ETC as a result of increased mitochondrial activity. We measured the oxygen consumption of H4IIEC3 cells treated with 400  $\mu\text{mol/L}$  PA to determine if ROS accumulation was associated with elevated mitochondrial metabolism. PA-treated cells were characterized by increased

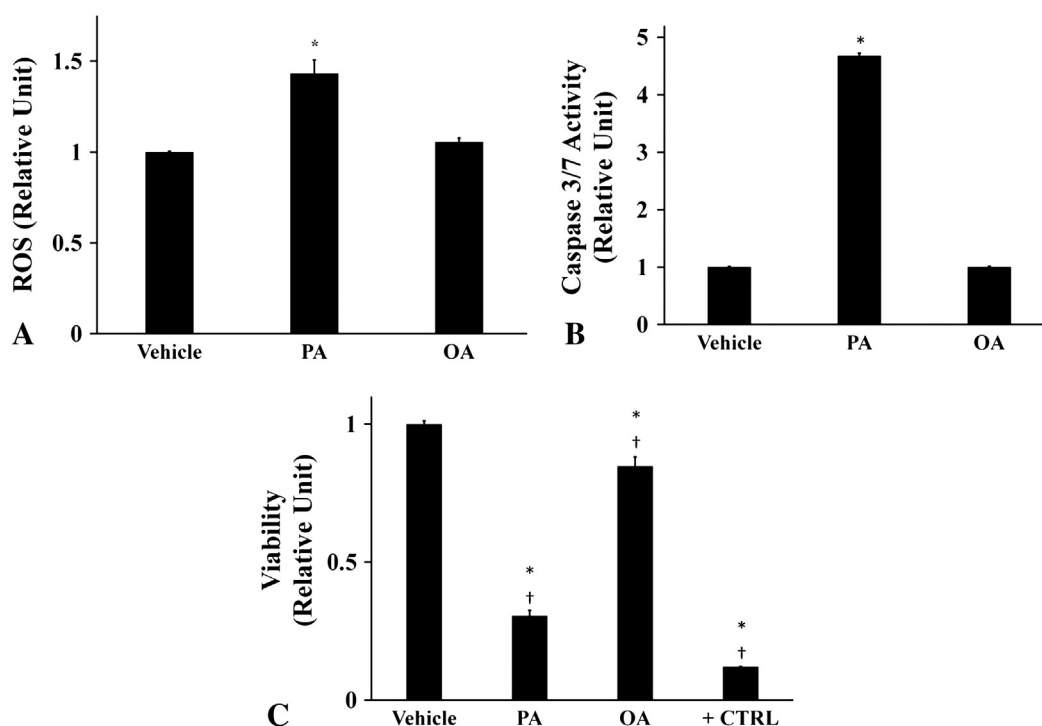


**Fig. 1 – Palmitate-induced lipotoxicity is characterized by time-dependent increases in ROS accumulation, caspase activation, and losses in cell viability.** H4IIEC3 rat hepatoma cells were incubated with 400  $\mu\text{mol/L}$  palmitate (PA), 400  $\mu\text{mol/L}$  oleate (OA), or 800  $\mu\text{mol/L}$  BSA (vehicle) for the indicated time periods. (A) Normalized ROS accumulation at 6-h time point measured by DCF fluorescence. (B) Caspase 3/7 activity at 12-h time point. (C) 24-h cell viability (resazurin reduction) after incubation with indicated treatments. Positive control cells (+CTRL) were treated with 70% ethanol for 30 min. Data represent mean  $\pm$  S.E.,  $n = 4$  for fluorescence assays; \*, different from vehicle,  $p < .05$ ; †, different from each other,  $p < .05$ .

oxygen consumption (Fig. 2). Cells treated with 400  $\mu\text{mol/L}$  OA had similar oxygen consumption rates as vehicle-treated cells. This result confirms that the elevated oxidative phenotype is unique to cells treated with SFA and that an equal load of MUFA is not sufficient to alter mitochondrial function.

### 3.3. Antioxidants restore viability by reducing palmitate-induced ROS accumulation without altering mitochondrial metabolism

Enhanced ROS accumulation has been proposed as playing a causative role in a variety of lipotoxic disorders. To determine if increased ROS levels were directly responsible for reducing cell viability in our system, H4IIEC3 cells were co-incubated with 400  $\mu\text{mol/L}$  PA and 5 mmol/L of the antioxidant *N*-acetyl cysteine (NAC). NAC co-treatment reduced ROS at 6 h (Fig. 3A), prevented markers of apoptosis at 12 h (Fig. 3B), and resulted in a proportional rescue in cell viability at 24 h (Fig. 3C). The antioxidant vitamin E produced similar reductions in lipotoxicity (Supplementary Fig. S2). The similar effects of both NAC and vitamin E, despite different mechanisms of ROS scavenging, suggest that NAC acts primarily through its antioxidant function to reduce lipotoxicity. Interestingly, NAC and PA co-treated H4IIEC3 cells had a similar oxygen uptake rate as cells treated with PA alone (Fig. 3D). This result indicates that palmitate-induced activation of mitochondrial metabolism is independent of ROS accumulation and apoptosis initiation.

### 3.4. Direct inhibition of mitochondrial oxidative metabolism suppresses palmitate-induced ROS generation and apoptosis

In a converse experiment, we sought to test whether a direct inhibitor of mitochondrial metabolism could effectively prevent the ability of palmitate to promote ROS accumulation and induce apoptosis. We applied 100  $\mu\text{mol/L}$  phenformin, a mitochondrial complex I antagonist, to H4IIEC3 cells in both the presence and absence of PA. Phenformin reduced PA-induced ROS generation at 6 h (Fig. 4A), caspase activation at 12 h (Fig. 4B), and long-term cell toxicity at 24 h (Fig. 4C) compared to cells treated with PA alone. (In these experiments, we measured PI fluorescence as an indicator of cell toxicity since mitochondrial inhibitors such as phenformin could interfere with accurate assessment of cell viability using resazurin-based dyes.) Experiments using the classical complex I inhibitor rotenone produced similar reductions in ROS accumulation and apoptosis in the presence of 400  $\mu\text{mol/L}$  PA, thus confirming our ability to rescue palmitate-induced apoptosis by inhibiting mitochondrial electron transport (Supplementary Fig. S3). To confirm that phenformin suppressed mitochondrial metabolism at the administered dose, we measured oxygen uptake by cells co-treated with PA and phenformin (Fig. 4D). The measurements confirmed that phenformin fully normalized oxygen uptake in the presence of palmitate, recapitulating the metabolic phenotype observed in vehicle-treated control cells.

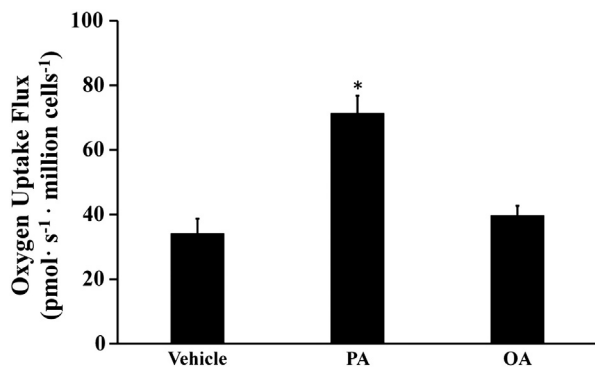


**Fig. 2 – Palmitate stimulates oxidative metabolism while oleate does not. Oxygen consumption measurements were performed on cells treated with vehicle, 400  $\mu\text{mol/L}$  palmitate (PA), and 400  $\mu\text{mol/L}$  oleate (OA) for three hours. Data represent mean  $\pm$  S.E.,  $n = 3$ ; \*different from vehicle,  $p < .05$ .**

### 3.5. Palmitate-induced ROS accumulation is independent of beta-oxidation

There are differing reports on the role of beta-oxidation in promoting *in vitro* lipotoxicity of hepatic cells [8,26]. To determine whether the observed ROS accumulation was due to a direct enhancement of beta-oxidation by palmitate

addition, H4IIEC3 cells were treated with 400  $\mu\text{mol/L}$  PA and 250  $\mu\text{mol/L}$  etomoxir. Etomoxir is a specific inhibitor of the rate-limiting carnitine palmitoyltransferase 1 (CPT-1) enzyme that is required to transport long-chain fatty acids across the mitochondrial membrane [27]. First, we confirmed that adding etomoxir to [9,10-<sup>3</sup>H(N)]palmitate-treated cells significantly attenuated beta-oxidation by measuring a decrease in <sup>3</sup>H<sub>2</sub>O production (Fig. 5A). To further confirm that etomoxir was effective at the selected concentration, we used AICAR to induce beta-oxidation in the presence of exogenous palmitate [28]. The effects of AICAR on beta-oxidation were completely reversed by addition of 250  $\mu\text{mol/L}$  etomoxir, confirming that this dose was effective at blocking CPT-1 in H4IIEC3 cells. Next, we observed that co-treatment with PA and etomoxir resulted in no significant change in ROS production in comparison to treatment with PA alone despite the observed reduction in beta-oxidation (Fig. 5B). Blocking beta-oxidation with etomoxir also did not prevent the appearance of markers of apoptosis (Fig. 5C, D).

To directly assess the contribution of palmitate toward supplying carbon for CAC intermediates, we treated H4IIEC3 rat hepatomas with [U-<sup>13</sup>C<sub>16</sub>]palmitate. Intracellular, non-protein-bound metabolites were extracted, derivatized, and analyzed by GC-MS to quantify <sup>13</sup>C-enrichment. If carbon from <sup>13</sup>C-labeled PA was fully oxidized in the CAC, it would enter the cycle initially as a fully labeled (M + 2) acetyl-CoA. This acetyl-CoA would then give rise to M + 2 labeled CAC intermediates such as

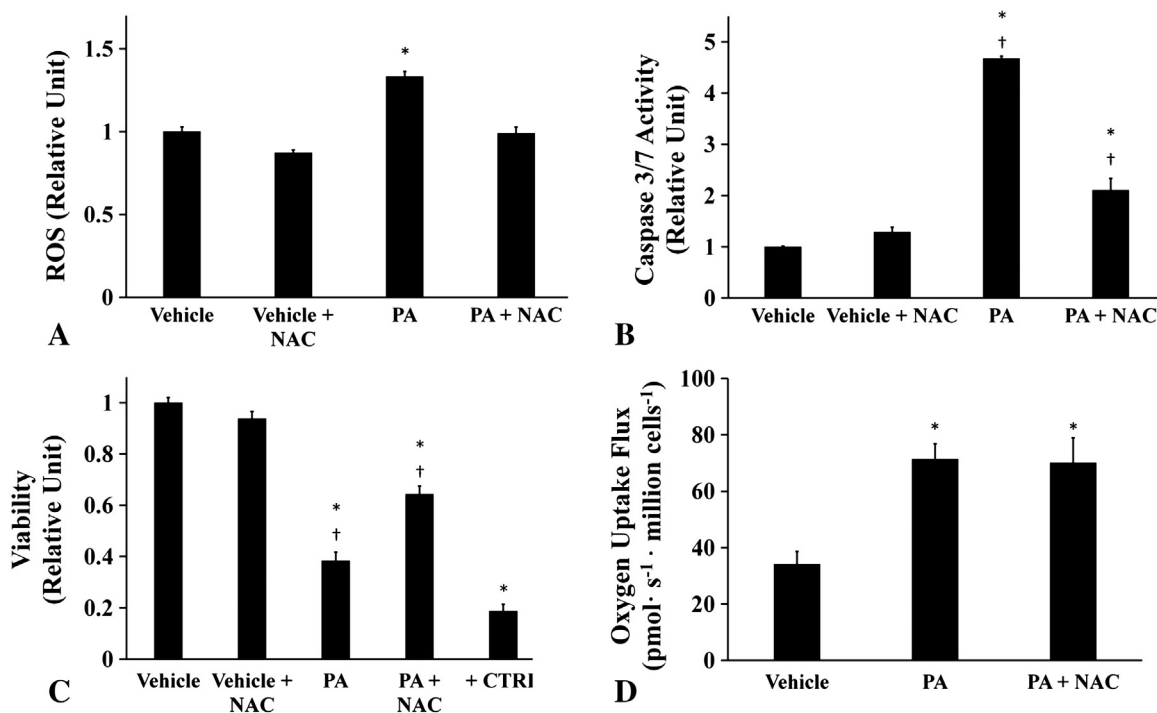


**Fig. 3 – Antioxidant treatment reduces intracellular ROS and partially rescues lipotoxic cell death without reversing palmitate-induced activation of oxidative metabolism. The antioxidant N-acetyl cysteine (NAC) was added at a concentration of 5 mmol/L to palmitate-treated (PA, 400  $\mu\text{mol/L}$ ) or BSA-treated (vehicle, 800  $\mu\text{mol/L}$ ) H4IIEC3 cells. (A) 6-h ROS accumulation measured by DCF fluorescence. (B) Caspase 3/7 activity at 12-h time point. (C) 24-h cell viability assessed by resazurin reduction. Positive control cells (+CTRL) were treated with 70% ethanol for 30 min. (D) Oxygen uptake measurements of NAC- and/or PA-treated cells. Data represent mean  $\pm$  S.E.,  $n = 4$  for all fluorescent assays,  $n = 3$  for oxygen uptake measurements; \* different from vehicle,  $p < .05$ ; † different from each other,  $p < .05$ .**

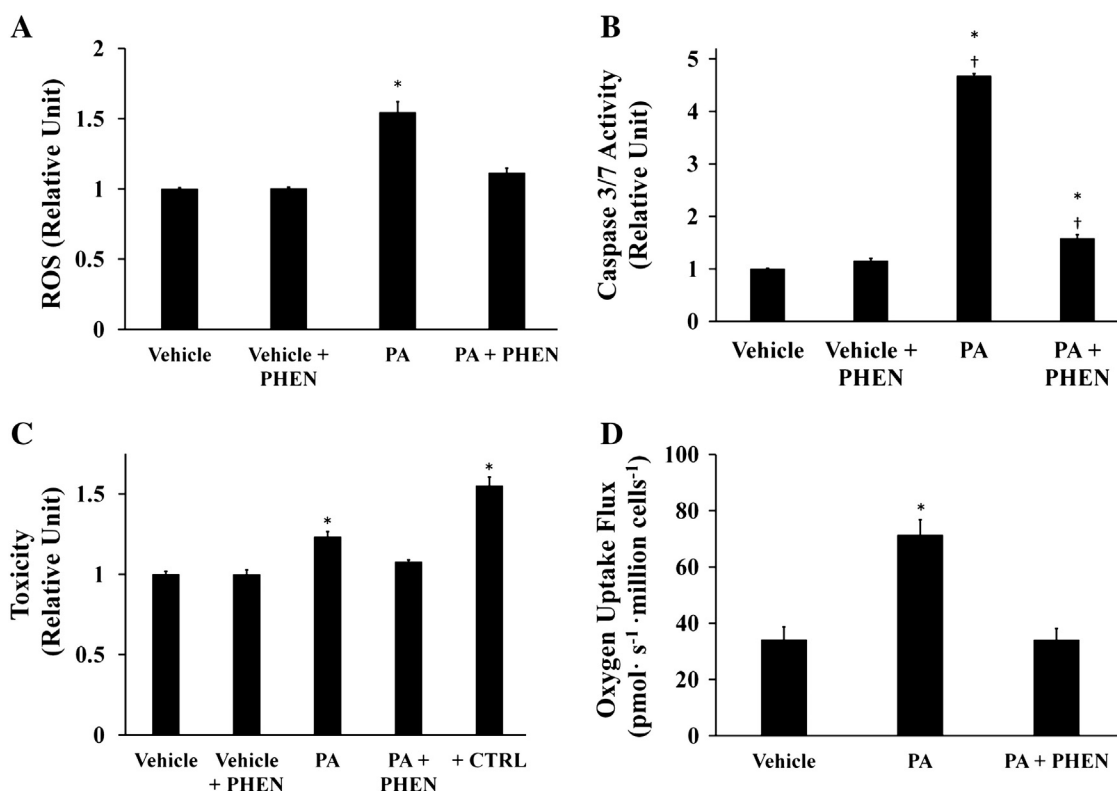


**Fig. 4 – Phenformin abolishes palmitate-induced ROS generation, mitochondrial activation, and apoptosis.** H4IIEC3 cells were co-treated with 100  $\mu\text{mol/L}$  phenformin (PHEN) and either 400  $\mu\text{mol/L}$  palmitate (PA) or 800  $\mu\text{mol/L}$  BSA (Vehicle) to examine the role of mitochondrial metabolism in ROS accumulation and apoptosis. (A) ROS levels at 6 h as measured by DCF fluorescence. (B) Caspase 3/7 activity at 12 h. (C) Cell toxicity at 24 h assessed by PI fluorescence. Positive control cells (+CTRL) were treated with 70% ethanol for 30 min. (D) Oxygen uptake measurements of PHEN- and/or PA-treated cells. Data represent mean  $\pm$  S.E.,  $n = 4$  for all fluorescent assays,  $n = 3$  for oxygen uptake measurements; \* different from vehicle,  $p < .05$ ; † different from each other,  $p < .05$ .

citrate and malate. Therefore, we analyzed ion fragments of citrate and malate for enrichment of  $M + 2$  mass isotopomers (Fig. 6A). However, we found little to no incorporation of  $^{13}\text{C}$ , suggesting that a negligible flux of palmitate carbon was directed into the CAC for complete oxidation.

### 3.6. Metabolic flux analysis identifies glutamine as a major fuel substrate for palmitate-induced mitochondrial activation

To identify sources of carbon flux into the CAC, we performed further isotope labeling studies by total replacement of medium glutamine with  $[\text{U-}^{13}\text{C}_5]\text{glutamine}$ . The average  $^{13}\text{C}$ -enrichment of a given metabolite therefore reflects the overall contribution of glutamine carbon to the metabolite pool relative to other unlabeled carbon sources (e.g., glucose or FFA). GC-MS analysis of  $^{13}\text{C}$  incorporation revealed that malate extracted from PA-treated cells approached 60% enrichment compared to approximately 30% enrichment in vehicle-treated cells (Fig. 6B). The addition of phenformin to PA-treated cells normalized the isotopic enrichment of malate to the level of control cells. On the other hand, NAC co-supplementation had only a minor effect on malate enrichment. Analysis of isotopic enrichment of glutamate revealed similar enrichment trends. Taken together, these data demonstrate that palmitate treatment is characterized by elevated glutamine consumption and increased entry of glutamine carbon into the CAC relative to other carbon sources.

Similar to the oxygen uptake measurements reported in Figs. 3D and 4D, phenformin co-treatment was able to reverse PA-induced alterations to glutamine metabolism while NAC co-treatment was not.

Next, we applied  $^{13}\text{C}$  MFA to simultaneously calculate 12 mitochondrial fluxes and their associated 95% confidence intervals by combining mass spectrometric measurements of  $^{13}\text{C}$  labeling with the previously measured oxygen consumption rates (Fig. 7A). H4IIEC3 cells treated with PA alone exhibited higher glutamine consumption, higher malic enzyme flux, and higher citrate synthase flux relative to vehicle-treated cells. Phenformin co-treatment effectively reduced most mitochondrial fluxes, including glutamine uptake and ETC activity. Cells co-treated with NAC and PA exhibited no reduction in mitochondrial metabolic fluxes, suggesting that the palmitate-induced metabolic alterations were not a consequence of elevated ROS and apoptosis initiation but instead were the result of upstream events in the lipotoxicity cascade that enhanced mitochondrial metabolic pathways.

Based on our  $^{13}\text{C}$  MFA calculations, we determined the difference between glycolytic pyruvate production and lactate excretion (Fig. 7B). We designate this difference as ‘net glycolysis’, since it represents the net amount of glycolytic carbon that enters the CAC for oxidation. If this value is positive, there is net contribution of glucose carbon to the mitochondrial metabolic pool. If negative, non-glucose carbon

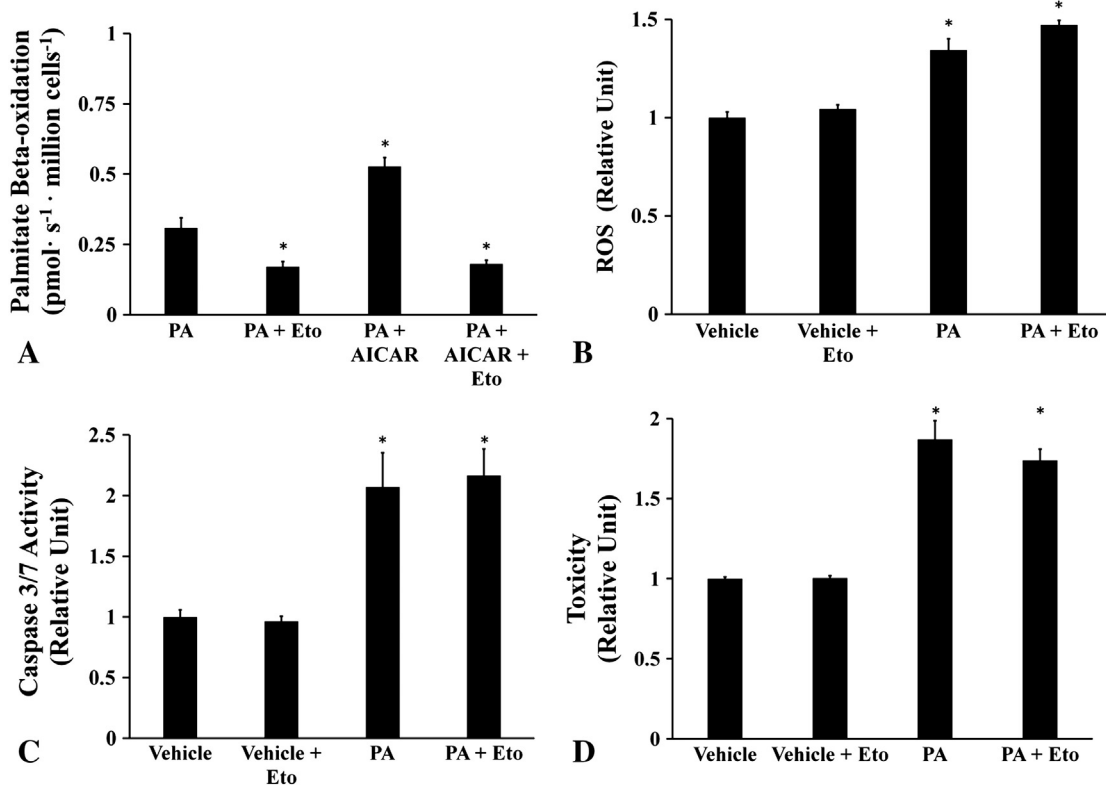


**Fig. 5 – Beta-oxidation does not fuel palmitate-induced ROS accumulation.** The CPT-1 inhibitor etomoxir (Eto) was added at a concentration of 250  $\mu\text{mol/L}$  to palmitate-treated (PA, 400  $\mu\text{mol/L}$ ) or BSA-treated (vehicle, 800  $\mu\text{mol/L}$ ) H4IIEC3 cells. (A) Beta-oxidation of [9,10- $^3\text{H(N)}$ ] palmitate assessed by  $^3\text{H}_2\text{O}$  production. 500  $\mu\text{mol/L}$  AICAR was used as a positive control. (B) ROS levels at 6 h measured by DCF fluorescence. (C) Caspase activity of cells treated with palmitate and etomoxir at 12 h. (D) Cell toxicity at 24 h assessed by PI fluorescence. Data represent mean  $\pm$  S.E.,  $n = 4$  for fluorescence assays, \* different from palmitate in (A), vehicle in (B, C, D),  $p < .05$ .

derived from the CAC is contributing to lactate production. For vehicle-treated cells, the net glycolytic rate was positive since more glucose carbon entered the pyruvate node than was excreted as lactate. Cells treated with PA, however, were characterized by a negative net glycolytic rate since glutamine entry to the CAC was elevated relative to glucose. Supplementing PA-treated cells with phenformin, but not NAC, effectively reversed this phenotype. Complete flux maps of all four treatments are shown in Fig. 8.

#### 4. Discussion

Understanding the molecular factors that control hepatic lipotoxicity is a critical step toward developing improved strategies to prevent and treat NAFLD and NASH. A reported feature of palmitate-induced lipotoxicity is increased oxidative stress due to intracellular ROS accumulation, which precedes the onset of apoptosis as indicated by DNA laddering, induction of caspases 3 and 7, and cytochrome C release [9,11,14,21,29]. However, the role of ROS in stimulating lipopoptosis appears to be cell-type dependent. For example, ROS accumulation is a critical event leading to apoptosis of palmitate-treated CHO cells [30], while palmitate-treated neonatal cardiomyocytes undergo apoptosis independently

of oxidative stress [31]. In our experiments, we measured a burst of ROS at approximately 6 h following palmitate administration, which was 25%–50% higher than cells treated with vehicle (BSA) alone. It has been shown previously in the H4IIEC3 cell line that similar increases in ROS can activate JNK stress pathways, which was sufficient to negatively affect insulin signaling [8]. We found that NAC co-treatment effectively normalized PA-induced ROS accumulation, significantly reduced caspase activation, and improved long-term cell viability, indicating that apoptosis initiation is dependent on ROS accumulation in H4IIEC3 cells.

Healthy cells continually produce ROS during mitochondrial oxidative phosphorylation and rely on their enzymatic machinery to manage ROS levels, thereby preventing toxic side effects. Elevated ROS can therefore occur due to either increased oxidative metabolism or deficient antioxidant defenses. To quantify rates of mitochondrial metabolism in palmitate-treated H4IIEC3 cells, we applied  $^{13}\text{C}$  MFA based on [U- $^{13}\text{C}_5$ ]glutamine tracing combined with measurements of oxygen consumption flux. Since mitochondria require oxygen to carry out oxidative phosphorylation, increased oxygen consumption is a direct measure of increased mitochondrial metabolism. Palmitate-treated cells exhibited a 2-fold increase in oxygen consumption rate and in most mitochondrial fluxes prior to ROS accumulation. However, NAC co-treatment

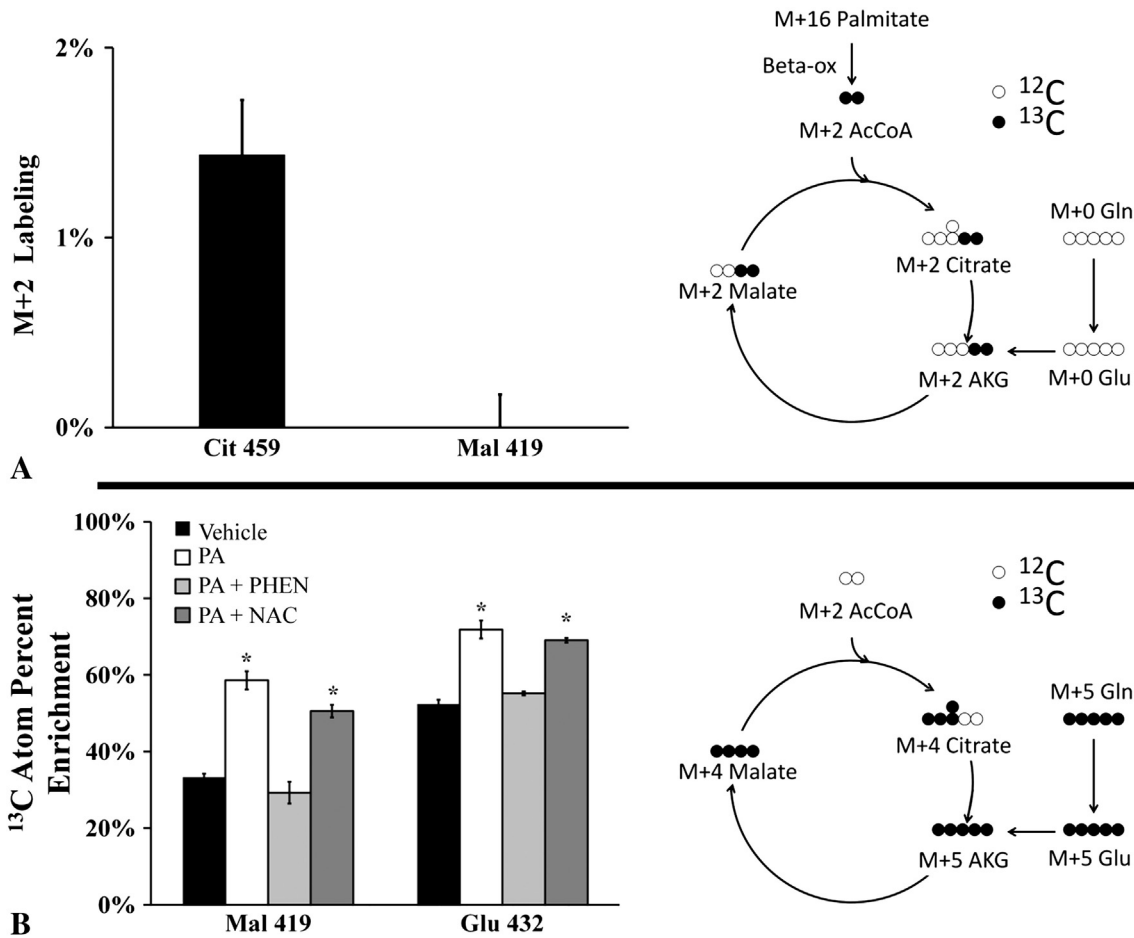


**Fig. 6 – Isotopic enrichment of mitochondrial metabolites.** Mass isotopomer distributions were corrected for natural isotope abundance using the method of Fernandez et al. [38]. (A) M + 2 mass isotopomer abundance resulting from incorporation of <sup>13</sup>C into malate and citrate following 6 h of incubation with 400 μmol/L [U-<sup>13</sup>C<sub>16</sub>]palmitate. Fully oxidized palmitate gives rise to M + 2 mass isotopomers as illustrated in the accompanying diagram. (B) Atom percent enrichment (APE) of cells incubated with [U-<sup>13</sup>C<sub>5</sub>]glutamine in combination with palmitate and phenformin or NAC co-treatments. APE was calculated using the formula  $APE = 100\% \times \sum_{i=0}^N \frac{M_i \times i}{N}$ , where N is the number of carbon atoms in the metabolite and M<sub>i</sub> is the fractional abundance of the i<sup>th</sup> mass isotopomer. The diagram illustrates the patterns of isotope incorporation derived from labeled glutamine after one turn of the CAC. Data represent mean ± S.E., n = 3; \* different from vehicle, p < .05.

did not affect palmitate-induced metabolic alterations, indicating that neither elevated ROS nor downstream apoptotic events contributed to mitochondrial activation. Instead, elevated mitochondrial metabolism appears to be an inherent consequence of palmitate overload that is independent of subsequent ROS accumulation and apoptosis initiation.

Next, we sought to determine whether accelerated mitochondrial metabolism is required for palmitate-induced ROS accumulation and apoptosis, or whether these events are primarily attributable to other causes such as failure of antioxidant defenses or activation of NADPH oxidases. To address this question, we employed the complex I antagonist phenformin to directly inhibit mitochondrial metabolism. Phenformin is a lipophilic derivative of the type-2 diabetes drug metformin, which shares the same mechanism of action [32,33]. Phenformin co-treatment reduced both ROS accumulation and oxygen uptake in PA-treated H4IIEC3 cells and normalized mitochondrial metabolic fluxes to levels charac-

teristic of vehicle-treated cells. Similar to NAC treatment, this reduction in mitochondria-derived ROS coincided with increased cell viability and decreased caspase activation. Therefore, elevated mitochondrial metabolism is required for ROS accumulation and caspase activation in our model of palmitate lipotoxicity.

Increased fatty acid beta-oxidation has been proposed as the primary fuel source responsible for lipotoxic ROS generation both *in vivo* [1,2] and in the H4IIEC3 cell line [8]. In our experiments with the same cell line, however, adding the CPT-1 inhibitor etomoxir to palmitate-treated H4IIEC3 cells had no effect on ROS accumulation or cell viability. These results reveal a novel facet of lipotoxicity in our system: mitochondria-derived ROS accumulation is independent of fatty acid beta-oxidation. We found little isotopic enrichment of CAC intermediates when H4IIEC3 cells were fed [U-<sup>13</sup>C<sub>16</sub>]palmitate, indicating that exogenous fatty acid was not being fully oxidized to CO<sub>2</sub>. To further investigate the fuel source driving

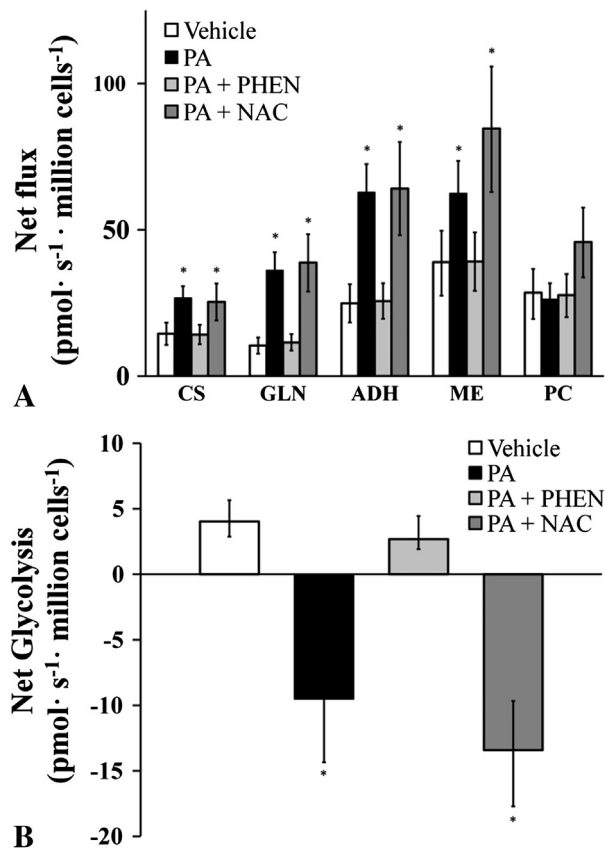


**Fig. 7** –  $^{13}\text{C}$  flux analysis of mitochondrial metabolism. Fluxes were calculated as described in the Methods section and further detailed in the Supplementary Materials. (A) Major CAC and anaplerotic fluxes of cells treated with BSA (Vehicle) or palmitate (PA) with and without NAC or phenformin (PHEN) co-treatments. Abbreviations: ADH, alpha-ketoglutarate dehydrogenase; CS, citrate synthase; GLN, glutamine uptake; ME, malic enzyme; PC, pyruvate carboxylase. (B) ‘Net glycolysis’ rate defined as the difference between glycolytic pyruvate production and lactate excretion. Error bars indicate 95% confidence intervals; \* different from vehicle,  $p < .05$ .

palmitate-induced mitochondrial activation, we relied on  $^{13}\text{C}$  MFA to map the flow of carbon entering the CAC from the major non-lipid substrates glucose and glutamine. We found that glutamine provided the primary fuel for elevated mitochondrial metabolism in the presence of palmitate, rather than fatty acid beta-oxidation, and that glutamine consumption could be reduced through co-treatment with phenformin but not NAC. These results demonstrate that ROS accumulation is a direct consequence of mitochondrial activation and can be reversed by inhibiting oxidative phosphorylation, which concomitantly suppresses entry of glutamine carbon into the CAC.

Our  $^{13}\text{C}$  MFA results match well with previous *in vivo*  $^2\text{H}/^{13}\text{C}$  NMR studies of NAFLD patients [2] and HFD fed mice [1], both of which reported an approximate 2-fold increase in CAC flux. This was associated with increased oxidative damage in livers of HFD fed mice [1]. The authors hypothesized that increased beta-oxidation was fueling the observed enhancement in CAC flux.

However, our *in vitro* observations supply an alternative hypothesis, which is that oxidation of non-lipid substrates can also contribute substantially to elevated CAC flux in hepatic lipotoxicity. It should be noted, however, that the *in vivo* flux studies were performed under fasting (i.e., gluconeogenic) conditions, whereas the conditions of our study were representative of a fed (i.e., glycolytic) state. Therefore, it is difficult to make direct quantitative comparisons between our data and those obtained from the prior *in vivo* studies.

Our findings suggest several intriguing questions for further study into the causes and consequences of mitochondrial dysregulation under conditions of FFA lipotoxicity. First, if the exogenous palmitate load does not directly fuel elevated CAC flux, what other effects of palmitate overexposure might lead to activation of mitochondrial oxidative metabolism? One possible hypothesis is that disruption of normal lipid metabolic pathways may lead to (i) production of lipid-derived signaling molecules or (ii) alteration of intracellular membrane homeostasis that subsequently activates mitochondrial metabolism. This may also involve activation of signaling proteins such as peroxisome proliferator-activated receptors (PPARs) that respond directly to lipid intermediates and can regulate expression of mitochondrial proteins. Although our study provides a detailed picture of metabolic flux rewiring in response to FFA treatments, it does not address the upstream cell signaling and transcriptional regulatory mechanisms that may play a role in mediating the observed metabolic alterations. Second, can direct inhibition of glutamine anaplerosis reverse the lipotoxic metabolic phenotype or will hepatic cells shift to other available carbon sources to maintain elevated CAC flux? Further investigation of both the upstream and downstream molecular events that control palmitate-induced mitochondrial activation in hepatic cells is clearly an important next step.

In summary, we have applied oxygen uptake measurements and  $^{13}\text{C}$  MFA to elucidate a critical role for mitochondrial dysregulation in mediating palmitate lipotoxicity of H4IIEC3 cells. We report that a) palmitate-induced metabolic dysregulation is independent of oxidative damage and apoptosis initiation, b) apoptosis is dependent on palmitate-induced metabolic alterations leading to elevated ROS accumulation, and c) glutamine, not fatty acid beta-oxidation, provides the carbon fuel for enhanced CAC flux in response to a palmitate load. Our model also highlights important differences between the protective effects of phenformin and NAC, both of which have direct *in vivo* relevance. Studies using non-diabetic methionine- and choline-deficient mouse models of NASH demonstrate that metformin has the potential to reduce inflammation after induction of liver injury [34]. Additionally, NAC supplementation of HFD fed Sprague–Dawley rats successfully prevented the appearance of many markers of elevated oxidative stress such as peroxidized lipid species [35]. However, this study reported that NAC did not reverse potential upstream activators of liver dysfunction such as steatosis and only partially restored glutathione levels. Clinically, the use of antioxidants as a treatment for NASH has met with varying degrees of success. For example, the antioxidant vitamin E has been explored as a potential therapy for persons with NASH. Treatment with vitamin E resulted in reduced liver injury in adults assessed by a reduction in serum alanine and aspartate aminotransferase

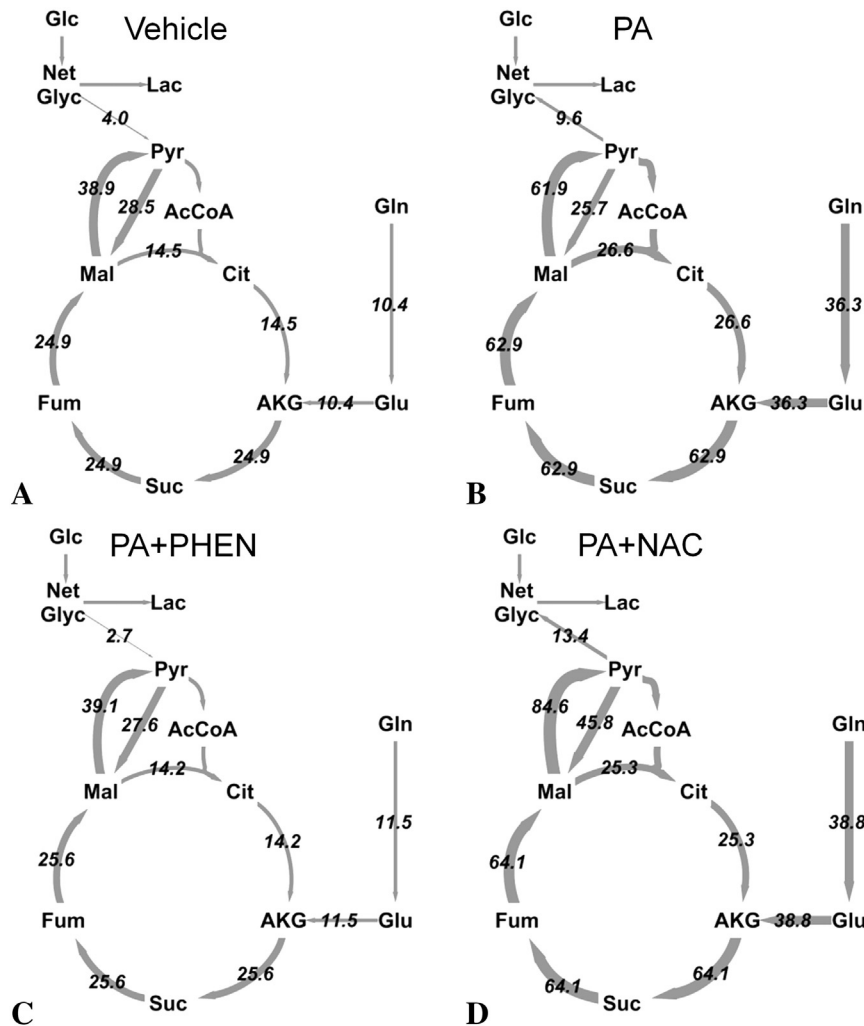


**Fig. 8 – Comparison of H4IIEC3 flux maps under various treatments examined in this study. Arrows are weighted according to flux values shown (pmol/million cells/s). (A) Vehicle-treated cells, (B) palmitate (PA) treated cells, (C) palmitate and phenformin (PA + PHEN) co-treated cells, (D) palmitate and NAC (PA + NAC) co-treated cells. Abbreviations: AcCoA, acetyl-CoA; AKG, alpha-ketoglutarate; Cit, citrate; Fum, fumarate; Glc, glucose; Glu, glutamate; Gln, glutamine; Lac, lactate; Mal, malate; Net Glyc, net glycolysis; Pyr, pyruvate; Suc, succinate.**

levels but did not improve fibrosis [36]. Interestingly, vitamin E trials in children with NASH report no improvements in alanine aminotransferase levels as a primary marker of disease but had improved NASH scores [37]. These prior *in vivo* studies highlight how antioxidants can treat some but not all symptoms of NASH, suggesting they do not fully restore normal redox homeostasis or block other upstream or parallel disease pathways. Improved understanding of the molecular determinants of lipotoxicity is therefore likely to suggest novel nutritional and/or pharmacologic interventions to combat the effects of NAFLD and to prevent its progression toward NASH.

**Author contributions**

R.A. Egnatchik performed and designed the experiments and wrote and edited the manuscript. A.K. Leamy performed the

beta-oxidation measurements and edited the manuscript. Y. Noguchi edited the manuscript and aided in experimental design. M. Shiota helped design the beta-oxidation measurements and edited the manuscript. J.D. Young wrote and edited the manuscript and aided in experimental design.

**Acknowledgments**

This research was supported by National Science Foundation (NSF) CAREER Award CBET-0955251 (to JDY) and the Vanderbilt Diabetes Research and Training Center (NIH DK020593). RAE was supported by the NSF Graduate Research Fellowship Program. We would like to thank Alyssa Hasty, Owen McGuinness, Richard O’Brien, and David Wasserman for critical readings of this manuscript prior to journal submission. Additionally, we would like to thank Wasserman lab members Ashley S. Williams and Louise Lantier for their

technical assistance with obtaining oxygen uptake measurements using the Oroboros Oxygraph-2K instrument.

### Conflict of interest

There is no conflict of interest to report.

### Appendix A. Supplementary data

Supplementary data to this article can be found online at <http://dx.doi.org/10.1016/j.metabol.2013.10.009>.

### REFERENCES

- [1] Satapati S, Sunny NE, Kucejova B, Fu X, He TT, et al. Elevated TCA cycle function in the pathology of diet-induced hepatic insulin resistance and fatty liver. *J Lipid Res* 2012;53:1080–92.
- [2] Sunny NE, Parks EJ, Browning JD, Burgess SC. Excessive hepatic mitochondrial TCA cycle and gluconeogenesis in humans with nonalcoholic fatty liver disease. *Cell Metab* 2011;14:804–10.
- [3] Samuel VT, Liu ZX, Qu X, Elder BD, Bilz S, et al. Mechanism of hepatic insulin resistance in non-alcoholic fatty liver disease. *J Biol Chem* 2004;279:32345–53.
- [4] Savage DB, Petersen KF, Shulman GI. Disordered lipid metabolism and the pathogenesis of insulin resistance. *Physiol Rev* 2007;87:507–20.
- [5] Sanyal AJ, Campbell-Sargent C, Mirshahi F, Rizzo WB, Contos MJ, et al. Nonalcoholic steatohepatitis: association of insulin resistance and mitochondrial abnormalities. *Gastroenterology* 2001;120:1183–92.
- [6] Serviddio G, Bellanti F, Tamborra R, Rollo T, Capitanio N, et al. Uncoupling protein-2 (UCP2) induces mitochondrial proton leak and increases susceptibility of non-alcoholic steatohepatitis (NASH) liver to ischaemia-reperfusion injury. *Gut* 2008;57:957–65.
- [7] Pessayre D, Fromenty B. NASH: a mitochondrial disease. *J Hepatol* 2005;42:928–40.
- [8] Nakamura S, Takamura T, Matsuzawa-Nagata N, Takayama H, Misu H, et al. Palmitate induces insulin resistance in H4IIEC3 hepatocytes through reactive oxygen species produced by mitochondria. *J Biol Chem* 2009;284:14809–18.
- [9] Noguchi Y, Young J, Aleman J, Hansen M, Kelleher J, et al. Effect of anaplerotic fluxes and amino acid availability on hepatic lipoapoptosis. *J Biol Chem* 2009;284:33425–36.
- [10] Malhi H, Bronk SF, Werneburg NW, Gores GJ. Free fatty acids induce JNK-dependent hepatocyte lipoapoptosis. *J Biol Chem* 2006;281:12093–101.
- [11] Pfaffenbach K, Gentile C, Nivala A, Wang D, Wei Y, et al. Linking endoplasmic reticulum stress to cell death in hepatocytes: roles of C/EBP homologous protein and chemical chaperones in palmitate-mediated cell death. *Am J Physiol-Endocrinol Metab* 2010;298:E1027–35.
- [12] Leamy AK, Egnatchik RA, Young JD. Molecular mechanisms and the role of saturated fatty acids in the progression of non-alcoholic fatty liver disease. *Prog Lipid Res* 2013;52:165–74.
- [13] Listenberger L, Ory D, Schaffer J. Palmitate-induced apoptosis can occur through a ceramide-independent pathway. *J Biol Chem* 2001;276:14890–5.
- [14] Wei Y, Wang D, Topczewski F, Pagliassotti M. Saturated fatty acids induce endoplasmic reticulum stress and apoptosis independently of ceramide in liver cells. *Am J Physiol-Endocrinol Metab* 2006;291:E275–81.
- [15] Listenberger L, Han X, Lewis S, Cases S, Farese R, et al. Triglyceride accumulation protects against fatty acid-induced lipotoxicity. *Proc Natl Acad Sci U S A* 2003;100:3077–82.
- [16] Gao D, Nong S, Huang X, Lu Y, Zhao H, et al. The effects of palmitate on hepatic insulin resistance are mediated by NADPH Oxidase 3-derived reactive oxygen species through JNK and p38MAPK pathways. *J Biol Chem* 2010;285:29965–73.
- [17] Adam-Vizi V, Chinopoulos C. Bioenergetics and the formation of mitochondrial reactive oxygen species. *Trends Pharmacol Sci* 2006;27:639–45.
- [18] Brookes PS, Yoon YS, Robotham JL, Anders MW, Sheu SS. Calcium, ATP, and ROS: a mitochondrial love-hate triangle. *Am J Physiol-Cell Physiol* 2004;287:C817–33.
- [19] Kamata H, Honda S, Maeda S, Chang L, Hirata H, et al. Reactive oxygen species promote TNF alpha-induced death and sustained JNK activation by inhibiting MAP kinase phosphatases. *Cell* 2005;120:649–61.
- [20] Srivastava S, Chan C. Hydrogen peroxide and hydroxyl radicals mediate palmitate-induced cytotoxicity to hepatoma cells: relation to mitochondrial permeability transition. *Free Radic Res* 2007;41:38–49.
- [21] Wei Y, Wang D, Gentile C, Pagliassotti M. Reduced endoplasmic reticulum luminal calcium links saturated fatty acid-mediated endoplasmic reticulum stress and cell death in liver cells. *Mol Cell Biochem* 2009;331:31–40.
- [22] Wiechert W, Mollney M, Isermann N, Wurzel W, de Graaf A. Bidirectional reaction steps in metabolic networks: III. Explicit solution and analysis of isotopomer labeling systems. *Biotechnol Bioeng* 1999;66:69–85.
- [23] Antoniewicz MR, Kelleher JK, Stephanopoulos G. Elementary metabolite units (EMU): a novel framework for modeling isotopic distributions. *Metab Eng* 2007;9:68–86.
- [24] Young J, Walther J, Antoniewicz M, Yon H, Stephanopoulos G. An elementary metabolite unit (EMU) based method of isotopically nonstationary flux analysis. *Biotechnol Bioeng* 2008;99:686–99.
- [25] Antoniewicz MR, Kelleher JK, Stephanopoulos G. Determination of confidence intervals of metabolic fluxes estimated from stable isotope measurements. *Metab Eng* 2006;8:324–37.
- [26] Srivastava S, Chan C. Application of metabolic flux analysis to identify the mechanisms of free fatty acid toxicity to human hepatoma cell line. *Biotechnol Bioeng* 2008;99:399–410.
- [27] Cook GA, Gamble MS. Regulation of carnitine palmitoyl-transferase by insulin results in decreased activity and decreased apparent *k<sub>i</sub>* values for malonyl-CoA. *J Biol Chem* 1987;262:2050–5.
- [28] Kaushik VK, Young ME, Dean DJ, Kurowski TG, Saha AK, et al. Regulation of fatty acid oxidation and glucose metabolism in rat soleus muscle: effects of AICAR. *Am J Physiol-Endocrinol Metab* 2001;281:E335–40.
- [29] Pagliassotti M, Wei Y, Wang D. Saturated fatty acids induce cytotoxicity in hepatocytes via effects on the endoplasmic reticulum. *Obes Res* 2005;13:A31.
- [30] Borradaile NM, Han X, Harp JD, Gale SE, Ory DS, et al. Disruption of endoplasmic reticulum structure and integrity in lipotoxic cell death. *J Lipid Res* 2006;47:2726–37.
- [31] Hickson-Bick DLM, Sparagna GC, Buja LM, McMillin JB. Palmitate-induced apoptosis in neonatal cardiomyocytes is not dependent on the generation of ROS. *Am J Physiol-Heart Circ Physiol* 2002;282:H656–64.
- [32] Hawley SA, Ross FA, Chevtzoff C, Green KA, Evans A, et al. Use of cells expressing gamma subunit variants to identify diverse mechanisms of AMPK activation. *Cell Metab* 2010;11:554–65.

- [33] Owen MR, Doran E, Halestrap AP. Evidence that metformin exerts its anti-diabetic effects through inhibition of complex 1 of the mitochondrial respiratory chain. *Biochem J* 2000;348: 607–14.
- [34] Kita Y, Takamura T, Misu H, Ota T, Kurita S, et al. Metformin prevents and reverses inflammation in a non-diabetic mouse model of nonalcoholic steatohepatitis. *Plos One* 2012;7.
- [35] Baumgardner JN, Shankar K, Hennings L, Albano E, Badger TM, et al. N-acetylcysteine attenuates progression of liver pathology in a rat model of nonalcoholic steatohepatitis. *J Nutr* 2008;138:1872–9.
- [36] Sanyal AJ, Chalasani N, Kowdley KV, McCullough A, Diehl AM, et al. Pioglitazone, vitamin E, or placebo for nonalcoholic steatohepatitis. *N Engl J Med* 2010;362:1675–85.
- [37] Lavine JE, Schwimmer JB, Van Natta ML, Molleston JP, Murray KF, et al. Effect of vitamin e or metformin for treatment of nonalcoholic fatty liver disease in children and adolescents. The TONIC randomized controlled trial. *JAMA* 2011;305:1659–68.
- [38] Fernandez CA, Des Rosiers C, Previs SF, David F, Brunengraber H. Correction of <sup>13</sup>C mass isotopomer distributions for natural stable isotope abundance. *J Mass Spectrom* 1996;31: 255–62.